Available online at www.sciencedirect.com
ScienceDirect
Nuclear Physics B Proceedings Supplement 00 (2014) 1–6
Nuclear Physics B Proceedings Supplement

B → DK Dalitz plot analyses for γ/ϕ_3 at Belle

Yoshiyuki Onuki

University of Tokyo,
Hongo 7-3-1, Bunkyo-ku, Tokyo, Japan

Abstract

We present γ/ϕ_3 measurements that use Dalitz analysis and the relevant updates with ADS and GLW method from Belle experiment at the KEKB asymmetric energy collider of 3.5 GeV positron and 8.5 GeV electron, in Japan. The combined value of the γ/ϕ_3 with GLW + ADS and Dalitz results is $\gamma/\phi_3 = 73^{+13}_{-15}[^\circ]$.

Keywords:
Belle, γ, ϕ_3, ADS, GLW, Dalitz, GGSZ

1. Introduction

The CP violation observed in the quark sector is explained by an irreducible complex phase in the Cabibbo-Kobayashi-Maskawa (CKM) matrix [1] in the Standard Model. One of the unitarity constraints of the CKM matrix is given by the equation $V_{ud}V^*_{ub} + V_{cd}V^*_{cb} + V_{td}V^*_{tb} = 0$ which represents a triagnle in the complex plane. The phase can be determined from measurements of the three angles and sides of the triangle. The angles are defined with respect to the CKM matrix elements as $\alpha/\phi_2 = \arg[-(V_{td}V^*_{Vtb})/(V_{ud}V^*_{ub})]$, $\beta/\phi_1 = arg[-(V_{cd}V^*_{cb})/(V_{td}V^*_{tb})]$ and $\gamma/\phi 3 = arg[-(V_{ud}V^*_{ub})/(V_{cd}V^*_{cb})]$.

The angle γ/ϕ_3 can be measured most precisely with the interference of two decay paths, $b \to c$ and $b \to u$ quark transition in $B \to DK$ decay [2]. The $B \to DK$ decay is only proceeds via the tree dominated diagrams shown in Fig. 1 hence the γ/ϕ_3 can be determined theoretically very clean. Precise direct determination of the angle γ/ϕ_3 in the CKM unitary trianle has been strongly demanded to set the anchor point of the CP violation in the Standard Model in order to search for the new physics phenomena observing as a discrepancy from the point.

The Belle experiment[3, 4, 5] is the B factory at the KEKB asymmetric energy collider of 3.5 GeV positron and 8.5 GeV electron; it had accumulated integrated luminosity of over 1 ab^{-1} (711 fb^{-1} on the $\Upsilon(4S)$, $\sim$ 100 fb^{-1} off resonance/energy scan and the other $\Upsilon(nS)$ resonances.).

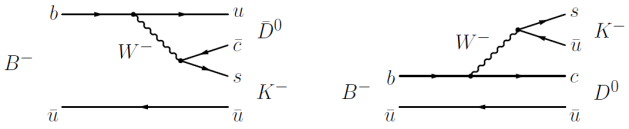

Figure 1: Diagram of $B^\pm \to DK^\pm$.

2. Analysis methods to extract γ/ϕ_3 information

Several methods to extract γ/ϕ_3 had been suggested so far: GLW [6], ADS [7], Dalitz(GGSZ) [8, 9] analyses.

2.1. GLW analysis

The GLW analysis uses D^0 and $\bar{D}^0$ decay into CP eigenstates such as K^+K^- or $K_S\pi^0$. The observables are a double ratio and an asymmetry defined as:

$$\begin{aligned} R_{CP\pm} &\equiv 2\frac{\Gamma(B^- \to D_{CP\pm}K^-) + \Gamma(B^- \to D_{CP\pm}K^-)}{\Gamma(B^- \to D^0K^-) + \Gamma(B^- \to \bar{D}^0K^-)} \\ &= 1 + r_B^2 \pm 2r_B \cos\delta_B \cos\phi_3 \end{aligned}$$

$$A_{CP\pm} \equiv \frac{\Gamma(B^- \to D_{CP\pm}K^-) - \Gamma(B^+ \to D_{CP\pm}K^+)}{\Gamma(B^- \to D_{CP\pm}K^-) + \Gamma(B^+ \to D_{CP\pm}K^+)} = \pm 2 r_B \sin\delta_B \sin\phi_3 / R_{CP\pm},$$

where $D_{CP\pm}$ is the D meson reconstructed in the CP-even (+) or CP-odd (-) final state, r_B is the ratio of amplitudes between $B^- \to \bar{D}^0 K^-$ and $B^- \to D^0 K^-$ defined as $r_B \equiv |A(B^- \to \bar{D}^0 K^-)/|A(B^- \to D^0 K^-)|$, and δ_B is the difference in strong phase for these amplitudes.

2.2. ADS analysis

ADS analysis uses $B^- \to D^{(*)}K^{(*)-}$ decays followed by the Cabibbo-favored (CF) and doubly Cabibbo-suppressed D^0 two body decays (DCS), where the interfering amplitudes have comparable magnitude. The CF (DCS) decay of the D meson that can be used for the ADS method are $D^0 \to K^-\pi^+$ ($D^0 \to K^+\pi^-$). The observables, double ratio and asymmetry, are defined as below

$$R_{ADS} \equiv \frac{\Gamma(B^- \to [f]_D K^-) + \Gamma(B^+ \to [\bar{f}]_D K^+)}{\Gamma(B^- \to [\bar{f}]_D K^-) + \Gamma(B^+ \to [f]_D K^+)} = r_B^2 + r_D^2 + 2 r_B r_D \cos(\delta_B + \delta_D)\cos\phi_3$$

$$A_{ADS} \equiv \frac{\Gamma(B^- \to [f]_D K^-) - \Gamma(B^+ \to [\bar{f}]_D K^+)}{\Gamma(B^- \to [f]_D K^-) + \Gamma(B^+ \to [\bar{f}]_D K^+)} = 2 r_B r_D \sin(\delta_B + \delta_D)\sin\phi_3 / R_{ADS},$$

where $r_D = |A(D^0 \to f)/A(\bar{D}^0 \to f)|$ and δ_D is the strong phase difference between $\bar{D}^0 \to f$ and $D^0 \to f$. Here f is the $K^+\pi^-$ two-body decay.

ADS for multi-body final state was proposed in Ref. [21], which leads to the modified double ratio and asymmetry

$$R_{ADS} = r_B^2 + r_D^2 + 2 r_B r_D R_F \cos(\delta_B + \delta_D^F)\cos\phi_3$$

$$A_{ADS} = 2 r_B r_D R_F \sin(\delta_B + \delta_D^F)\sin\phi_3 / R_{ADS}$$

where R_F and δ_D^F are the coherence factor for the DCS multi-body decay $D \to F$ and the average strong-phase difference as defined below, respectively. The coherence factor takes a value [0,1] depending on the Dalitz structure of the decay.

$$r_D^2 = \frac{\Gamma(D^0 \to F)}{\Gamma(D^0 \to \bar{F})} = \frac{\int d\mathbf{m} \mathcal{A}_{DCS}^2(\mathbf{m})}{\int d\mathbf{m} \mathcal{A}_{CF}^2(\mathbf{m})},$$

$$R_F e^{i\delta_D^F} = \frac{\int d\mathbf{m} \mathcal{A}_{DCS}(\mathbf{m}) \mathcal{A}_{CF}(\mathbf{m}) e^{i\delta(\mathbf{m})}}{\sqrt{\int d\mathbf{m} \mathcal{A}_{DCS}^2(\mathbf{m}) \int d\mathbf{m} \mathcal{A}_{CF}^2(\mathbf{m})}},$$

where $\mathcal{A}_{DCS}(\mathbf{m})$ and $\mathcal{A}_{CF}(\mathbf{m})$ are the DCS and CF amplitudes, respectively. The $\delta(\mathbf{m})$ is the strong phase. The $\mathbf{m}$ represents the point in the D decay Dalitz plane.

2.3. Model-dependent Dalitz analysis

Dalitz analysis with D meson decay into the multi-body decay is the most promissing way to extract the γ/ϕ_3 information. The model-dependent Datliz analysis in Belle uses the isobar model [10] which assume that the three-body decay of the D meson proceeds through the intermediate two-body resonances. The total amplitude over the Dalitz plot can be represented as the sum of two amplitudes for D^0 and $\bar{D}^0$ decays into the same final state $K_S h^+ h^-$ as below [11].

$$f_{B^+} = f_D(m_+^2, m_-^2) + r_B e^{\pm i\phi_3 + i\delta_B} f_D(m_-^2, m_+^2),$$

where $m_+^2 = m_{K_S h^+}^2$, $m_-^2 = m_{K_S h^-}^2$. The $f_D(m_+^2, m_-^2)$ consists of the sum of intermediates two-body amplitudes and a single non-resonant amplitude as follows.

$$f_D(m_+^2, m_-^2) = \sum_{j=1}^{N} a_j e^{i\xi_j} \mathcal{A}_j(m_+^2, m_-^2) + a_{NR} e^{i\xi_{NR}}$$

Where a_j and ξ_j are the amplitude and phase of the matrix element, $\mathcal{A}_j$ is the matrix element of the j-th resonance, and a_{NR} and ξ_{NR} are the amplitude and phase of the non-resonant component. The $r_B e^{\pm i\phi_3 + i\delta_B}$ can be converted to the Cartesian parameters $x_\pm = r_B \cos(\pm\phi_3 + \delta)$ and $y_\pm = r_B \sin(\pm\phi_3 + \delta)$. The $x_\pm$ and $y_\pm$ are the actual fitted parameters. The uncertainty on the assumed amplitudes is included in the measurement.

2.4. Model-independent Dalitz analysis

A new technique using a model-independent binned Dalitz method [12, 13] is reported by Belle [29] using strong-phase difference information obtained from quantum-correlated Dalitz plots by CLEO-c [30] to replace the model uncertainty is replaced by the measured strong-phase difference uncertainty, which scales with the statistics of charm factories. The model-independent method requires the Dalitz plot divided into $2N$ bins symmetrically under the exchange $m_-^2 \leftrightarrow m_+^2$. The bin index i ranges from $-N$ to N excluding 0. The expected number of events in i-th bin of the Dalitz plot of the D meson from $B^\pm \to DK^\pm$ is

$$N_i^\pm = h_B[K_{\pm i} + r_B^2 K_{\mp i} + 2\sqrt{K_i K_{-i}}(x_\pm c_i \pm y_\pm s_i)],$$

where h_B is a normalization constant and K_i is the number of events in the i-th bin of the $K_S^0\pi^+\pi^-$ Dalitz plot of the D meson in a flavor eigenstate. The c_i and s_i include information about the cosine and sine of the phase difference averaged over the bin and are determined from CLEO-c data.

3. Current results from Belle

3.1. GLW results

Belle measured the GLW observables with the final data set of $772 \times 10^6 B\bar{B}$ pairs [14, 15] shown in Table 1. The reconstructed modes are $B^\pm \to DK^\pm$ and $B^\pm \to D^*K^\pm$ followed by $D^* \to D\pi^0$ and $D^* \to D\gamma$. The reconstructed CP eigen modes are K^+K^- and $\pi^+\pi^-$ for CP-even, and $K_S\pi^0$ and $K_S\eta$ for CP-odd. These results are consistent with the results of BaBar [16, 17] and LHCb [20] in CP-even modes which dominates the precision now. As for the CP-odd modes, these are still unique inputs from B-factories. Fig. 2 shows the ΔE distributions at the energy difference for the $B^\pm \to D_{CP+}K^\pm$ modes.

$B^\pm \to DK^\pm$		
R_{CP+}	=	$1.03 \pm 0.07 \pm 0.03$
R_{CP-}	=	$1.13 \pm 0.09 \pm 0.05$
A_{CP+}	=	$0.29 \pm 0.06 \pm 0.02$
A_{CP-}	=	$-0.12 \pm 0.06 \pm 0.01$
$B^\pm \to D^*K^\pm$		
R_{CP+}	=	$1.19 \pm 0.13 \pm 0.03$
R_{CP-}	=	$1.03 \pm 0.13 \pm 0.03$
A_{CP+}	=	$-0.14 \pm 0.10 \pm 0.01$
A_{CP-}	=	$0.22 \pm 0.11 \pm 0.01$

Table 1: GLW results for $B^\pm \to DK^\pm$ and $D^*K^\pm$ followed by $D^* \to D\pi^0$ and $D^* \to D\gamma$.

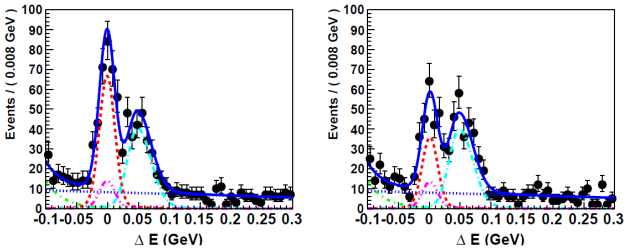

Figure 2: Signals in $B^- \to D_{CP+}K^-$ (left) and $B^+ \to D_{CP+}K^+$ (right) ΔE distribution. The points with error bars represent data while the total best-fit projection is shown with the solid blue curve, for which the components are shown with thicker dashed red (DK signal), dashed light blue ($D\pi$), dashed dot green ($B\bar{B}$ background), and dotted blue (combinatorial background) lines.

3.2. ADS results

ADS analysis of $B^\pm \to DK^\pm$ followed by $D \to K\pi$ is performed using full data set of Belle and achieved first evidence for an ADS signal with 4.1σ[18]. In addition, $D \to K\pi$ modes from $B^\pm \to D^*K^\pm$ followed by $D^* \to D\pi^0$ and $D^* \to D\gamma$ are also measured[14]. These results are summarized in Table 2 and are in good agreement with the BaBar [19] and LHCb [20] in $B^\pm \to DK^\pm$ followed by $D \to K\pi$. Fig. 3 shows the ΔE distributions of the observed $B^\pm \to DK^\pm$ modes.

$B^\pm \to DK^\pm, D \to K\pi$		
R_{ADS}	=	$0.0163\ ^{+0.0044\ +0.0007}_{-0.0041\ -0.0013}$
A_{ADS}	=	$-0.39\ ^{+0.26\ +0.04}_{-0.28\ -0.03}$
$B^\pm \to D^*K^\pm, D^* \to D\pi^0, D \to K\pi$		
R_{ADS}	=	$0.010\ ^{+0.008\ +0.001}_{-0.007\ -0.002}$
A_{ADS}	=	$0.4\ ^{+1.1\ +0.2}_{-0.7\ -0.1}$
$B^\pm \to D^*K^\pm, D^* \to D\gamma, D \to K\pi$		
R_{ADS}	=	$0.036\ ^{+0.014}_{-0.012} \pm 0.002$
A_{ADS}	=	$-0.51\ ^{+0.33}_{-0.29} \pm 0.08$

Table 2: ADS results for $B^\pm \to D^{(*)}K^\pm$.

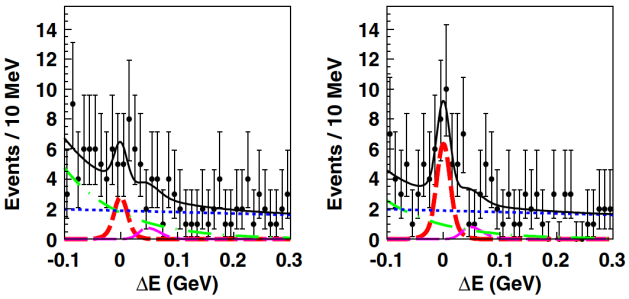

Figure 3: Signals in $B^- \to DK^-$ followed by $D \to K^+\pi^-$(left) and $B^+ \to DK^+$ followed by $D \to K^-\pi^+$(right) at ΔE distributions. The points with error bars represent data while the total best-fit projection is shown with the solid black curve. The components are shown with thicker dashed red (DK signal), thinner dashed magenta ($D\pi$), dashed dot green ($B\bar{B}$ background), and dotted blue ($q\bar{q}$ background) lines.

Belle also performed an ADS analysis for neutral $B^0 \to DK^{*0}$ decays, followed by $K^{*0} \to K^+\pi^-$ with the full data set. The results are shown in Table 3 [22]. In this mode, a factor, k, and average strong-phase difference is introduced in the R_{ADS}, A_{ADS} [23]

$$\begin{aligned} R_{ADS} &= r_S^2 + r_D^2 + 2kr_S r_D \cos(\delta_S + \delta_D)\cos\phi_3 \\ A_{ADS} &= 2kr_S r_D \sin(\delta_S + \delta_D)\sin\phi_3 / R_{ADS} \end{aligned}$$

with

$$r_S^2 \equiv \frac{\Gamma(B^0 \to D^0K^+\pi^-)}{\Gamma(B^0 \to \bar{D}^0K^+\pi^-)} = \frac{\int d\mathbf{p}\mathcal{A}^2_{b\to u}(\mathbf{p})}{\int d\mathbf{p}\mathcal{A}^2_{b\to c}(\mathbf{p})},$$

$$ke^{i\delta_{D_S}} \equiv \frac{\int d\mathbf{p}\mathcal{A}_{b\to c}(\mathbf{p})\mathcal{A}_{b\to u}(\mathbf{p})e^{i\delta(\mathbf{p})}}{\sqrt{\int d\mathbf{p}\mathcal{A}^2_{b\to c}(\mathbf{p})\int d\mathbf{p}\mathcal{A}^2_{b\to u}(\mathbf{p})}},$$

where $A_{b\to c}(\mathbf{p})$ and $A_{b\to u}(\mathbf{p})$ are the magnituxdes of the amplitudes for $b \to c$ and $b \to u$ transitions, respectively. The $\delta(\mathbf{p})$ is the relative strong phase. The $\mathbf{p}$ indicates the position in the $DK^+\pi^-$ Dalitz plane. The value of r_S is expected to be around 0.4, estimated from $|V_{ub}V^*_{cs}|/|V_{cb}V^*_{us}|$, and depends on the strong interaction effect. The factor k is expected to be around 0.95 [24]. This mode may have a larger value of R_{ADS} than that of charged modes.

$B^0 \to DK^{*0}, D \to K\pi, K^{*0} \to K^+\pi^-$		
R_{ADS}	=	$0.045\ ^{+0.056\ +0.028}_{-0.050\ -0.018}$
R_{ADS}	<	0.16 at 95% C.L.

Table 3: ADS results for $B^0 \to DK^{*0}$.

The decay channel $B^- \to DK^-$ followed by $D \to K^-\pi^+\pi^0$ has significantly larger branching fraction ($Br(D \to K^-\pi^+\pi^0) = 13.9 \pm 0.5\%$) than the $B \to K^-\pi^+$ ($Br(D \to K^-\pi^+) = 3.89 \pm 0.05\%$). Belle measured this mode and found the first evidence of a suppressed signal in this mode with a significance of 3.2σ as shown in Table 4 and Fig. 4 [25]. CLEO-c also measured the coherence factor $R_{K\pi\pi^0}$ and the average strong-phase difference $\delta_D^{K\pi\pi^0}$ with quantum-correlated $D\bar{D}$ decays at the $\psi(3770)$ resonance[26, 27]. The measured coherence factor 0.82 ± 0.07 gives comparable sensitivity with Dalitz analysis.

$B^\pm \to DK^\pm, D \to K\pi\pi^0$		
R_{ADS}	=	$0.0198 \pm0.0062 \pm0.0024$
A_{ADS}	=	$0.41 \pm0.30 \pm0.05$

Table 4: ADS results for $B^\pm \to DK^\pm, D \to K\pi\pi^0$.

3.3. Dalitz results

Currently the most precise determination of γ/ϕ_3 has been performed with Dalitz method.

The γ/ϕ_3 results of an model-dependent unbinned Dalitz method applied for $B^\pm \to DK^\pm$ and $B^\pm \to D^*K^\pm$ followed by $D^* \to D\gamma/\pi^0$ and $D \to K_S\pi\pi$ using 657 million events [28] are summarized in Table 5. Here the 3rd error is the model uncertainty related to the isobar model. Though this analysis observed evidence for direct CP violation with a significance of 3.5σ, the precision is almost dominated by the model uncertainty.

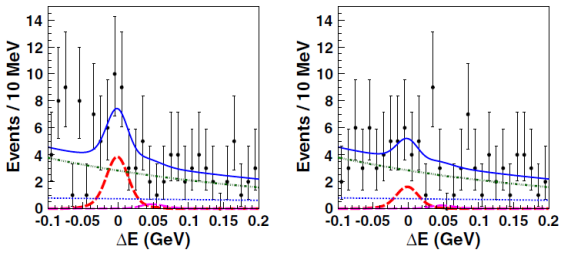

Figure 4: Signals in $B^- \to DK^-$ followed by $D \to K^+\pi^-\pi^0$(left) and $B^+ \to DK^+$ followed by $D \to K^-\pi^+\pi^0$(right) ΔE distributions. The points with error bars represent data while the total best-fit projection is shown with the solid blue curve. The components are shown with thicker dashed red (DK signal), thinner dashed magenta ($D\pi$), dashed dot green ($B\bar{B}$ background), and dotted blue ($q\bar{q}$ background) lines.

$B^\pm \to DK^\pm, D \to K_S\pi\pi$		
$\gamma/\phi_3[^\circ]$	=	$78.4\ ^{+10.8}_{-11.6} \pm3.6 \pm8.9$
r_{DK}	=	$0.161\ ^{+0.040}_{-0.038} \pm0.011\ ^{+0.050}_{-0.010}$
r_{D*K}	=	$0.196\ ^{+0.073}_{-0.072} \pm0.013\ ^{+0.062}_{-0.012}$
$\delta_{DK}[^\circ]$	=	$137.4\ ^{+13.0}_{-15.7} \pm4.0 \pm22.9$
$\delta_{D*K}[^\circ]$	=	$341.7\ ^{+18.6}_{-20.9} \pm3.2 \pm22.9$

Table 5: Model-dependent Dalitz results for $B^\pm \to D^{(*)}K^\pm$, $D^* \to D\gamma/\pi^0$, $D \to K_S\pi\pi$.

Belle reported the first γ/ϕ_3 measurement with the model-dependent Dalitz method for $B^\pm \to DK^\pm$ followed by $D \to K_S\pi\pi$ using full data [29]. The measurements are summarized in Table 6. Here the 3rd error is the uncertainty of the strong phase determination in the Dalitz plane studied by CLEO-c experiment based on 818 pb^{-1} at $\Upsilon(3770)$ [30]. Fig. 5 shows the obtained (x, y) parameters. Fig. 6 shows the obtained r_B and ϕ_3 dependence. Fig. 7 shows the obtained δ_B and ϕ_3 dependence.

$B^\pm \to DK^\pm, D \to K_S\pi\pi$		
$\gamma/\phi_3[^\circ]$	=	$77.3\ ^{+15.1}_{-14.9} \pm4.1 \pm4.3$
r_{DK}	=	$0.145 \pm0.030 \pm0.010 \pm0.011$
$\delta_{DK}[^\circ]$	=	$129.9 \pm15.0 \pm3.8 \pm4.7$

Table 6: Model-independent Dalitz results for $B^\pm \to DK^\pm$, $D \to K_S\pi\pi$.

4. Conclusion

The value of γ/ϕ_3 can be obtained in a theoretically-clean manner using tree-dominated decays. Belle obtained $\gamma/\phi_3 = 73^{+13}_{-15}[^\circ]$ with a combination of ADS,

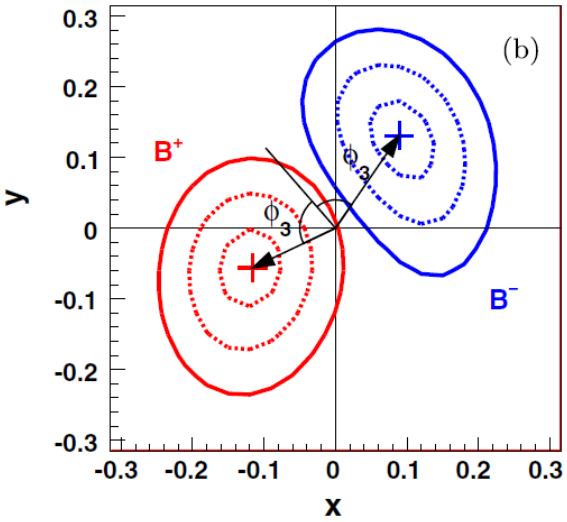

Figure 5: Obtained (x, y) parameters with model-independent Dalitz analysis. Each contour shows 1,2 and 3 σ confidence level.

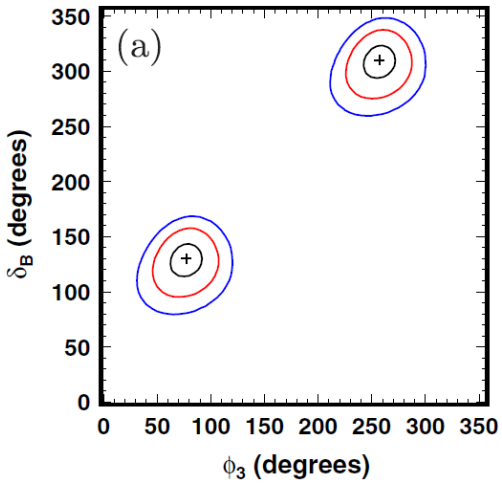

Figure 7: Obtained constraints of (δ_B, ϕ_3) with model-independent Dalitz analysis. Each contour shows 1,2 and 3 σ confidence level.

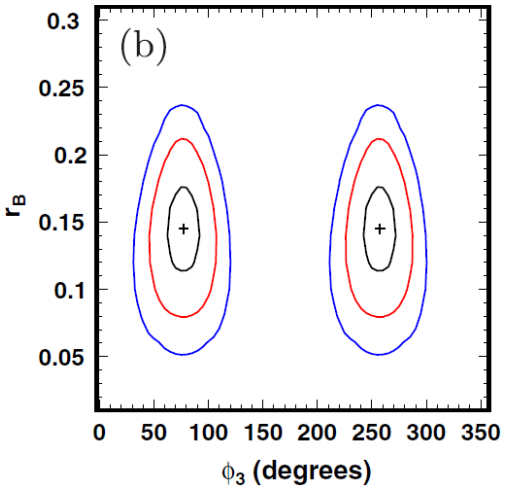

Figure 6: Obtained constraints of (r_B, ϕ_3) with model-independent Dalitz analysis. Each contour shows 1,2 and 3 σ confidence level.

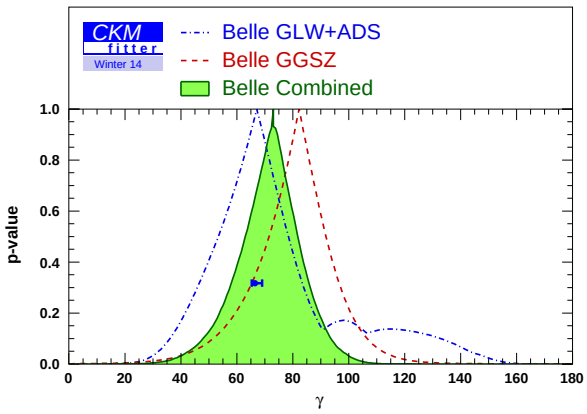

Figure 8: Constraints on γ/ϕ_3 from Belle measurements on $D^{(*)}K^{(*)}$(GLW+ADS) and Dalitz(GGSZ) analyses. $\gamma/\phi_3 = 73^{+13}_{-15}[^\circ]$

GLW and Dalitz results [31]. The most precise determination of γ/ϕ_3 is brought from the the model-dependent and newly developed model-independent Dalitz analyses. The model-independent analysis pushed down the uncertainty limitation and replaced to model-related uncertainty with statistical strong-phase uncertainty which can be reduced by BESIII experiment. In addition, recent ADS and GLW applications to various modes gives a determination that is competitive with the Dalitz analysis ; this can be seen in Fig. 8. With important input from charm-factories, B-factories and LHCb open up the possibilities of much higher precision determination of γ/ϕ_3 in the near future.

References

[1] N. Cabibbo, Phys. Rev. Lett. **10**, 531 (1963); M. Kobayashi and T. Maskawa, Prog. Theor. Phys. **49**, 652 (1973).
[2] A. B. Carter and A. I. Sanda, Phys. Rev. Lett. **45**, 952 (1980); I. I. Bigi and A. I. Sanda, Phys. Lett. B **211**, 213 (1988).
[3] A. Abashian *et al.* (Belle Collaboration), Nucl. Instrum. Methods Phys. Res., Sect. A **479**, 117 (2002).
[4] J. Brodzicka *et al.* (Belle Collaboration), Prog. Theor. Exp. Phys. 2012 (2012) 04D001.: arXiv:1212.5342[hep-ex].
[5] A. J. Bevan *et al*, arXiv:1406.6311[hep-ex].
[6] M. Gronau, D. London, D. Wyler, Phys. Lett. B **253**, 483 (1991); M. Gronau, D. London, D. Wyler, Phys. Lett. B **265**, 172 (1991).
[7] D. Atwood, I. Dunietz, A. Soni, Phys. Rev. Lett. **78**, 3257 (1997); Phys. Rev. D **63** 036005 (2001).
[8] A. Giri, Yu. Grossman, A. Soffer, J. Zupan, Phys. Rev. D **68**, 054018 (2003).
[9] A. Bondar. Proceedings of BINP Special Analysis Meeting on Datliz Analysis, 24-26 Sep. 2002, unpublished.
[10] S. Kopp *et al.* (CLEO Collaboration), Phys. Rev. D **63**, 092001 (2001); H. Muramatsu *et al.* (CLEO Collaboration), Phys. Rev. Lett. **89**, 251802 (2002); **90**, 059901 (2003).
[11] A. Poluektov *et al.* (Belle Collaboration), Phys. Rev. D **73**, 112009 (2006).
[12] A. Bondar and A. Poluektov, Eur. Phys. J. C **47**, 347-353 (2006).
[13] A. Bondar and A. Poluektov, Eur. Phys. J. C **55**, 51-56 (2008).
[14] Belle Collaboration, preliminary results presented at Lepton Photon 2011. BELLE-CONF-1112.
[15] K. Trabelsi *et al.* (Belle Collaboration), arXiv:1301.2033[hep-ex].
[16] P.del Amo Sanchez *et al.* (BaBar Collaboration), Phys. Rev. D **82**, 072004 (2010).
[17] B. Aubert *et al.* (BaBar Collaboration), Phys. Rev. D **78**, 092002 (2008).
[18] Y. Horii *et al.* (Belle Collaboration), Phys. Rev. Lett. **106**, 231803 (2011).
[19] P.del Amo Sanchez *et al.* (BaBar Collaboration), Phys. Rev. D **82**, 072006 (2010).
[20] R. Aaij *et al.* (LHCb Collaboration), Phys. Lett. B **712**, 203 (2012).
[21] D. Atwood, A. Soni, Phys. Rev. D **68**, 033003 (2003).
[22] K. Negishi *et al.* (Belle Collaboration), Phys. Rev. D **86**, 011101(R) (2012).
[23] M. Gronau, Phys. Lett. B **557**, 198 (2003).
[24] B. Aubert *et al.* (BaBar Collaboration), Phys. Rev. D **79**, 072003 (2009).
[25] M. Nayak *et al.* (Belle Collaboration), Phys. Rev. D **88**, 091104 (2013).
[26] N. Lowrey *et al.* (Belle Collaboration), Phys. Rev. D **80**, 031105(R) (2009).
[27] J. Libby *et al*, Phys. Lett. B **731**, 197-203 (2014).
[28] A. Poluektov *et al.* (Belle Collaboration), Phys. Rev. D **81**, 112002 (2010).
[29] H. Aihara *et al.* (Belle Collaboration), Phys. Rev. D **85**, 112014 (2012).
[30] R. A. Briere *et al.* (CLEO Collaboration), Phys. Rev. D **80**, 032002 (2009);J. Libby *et al.* (CLEO Collaboration), Phys. Rev. D **82**, 112006 (2010).
[31] J. Charles *et al.* (CKMfitter Group), Eur. Phys. J. **C41**, 1 and online update at http://ckmfitter.in2p3.fr/.